

Helicons in indium single crystals in the intermediate state

I. P. Krylov

Institute of Physics Problems, USSR Academy of Sciences
(Submitted May 11, 1976)

Zh. Eksp. Teor. Fiz. 71, 1620–1633 (October 1976)

Free and forced helicon oscillations in high-purity indium single crystals are investigated experimentally. The dependence of the helicon dispersion law and damping on the magnitude and direction of the magnetic field is studied. In agreement with the basic law of macroscopic electrodynamics, the dispersion law and damping of helicons are found to be independent of the structure of the intermediate-state domains. The resonance frequency of the oscillations in the plate do not depend on the concentration of the normal phase and decrease with inclination of the magnetic field relative to the normal to the plate surface. The damping of helicons in the intermediate state is independent of the inclination of the magnetic field. These facts are in agreement with Andreev's theory. (Zh. Eksp. Teor. Fiz. 51, 1510, 1966; Sov. Phys. JETP. 24 1019, 1967).

PACS numbers: 75.60.Fk, 76.90.+d

In 1966, Andreev derived the equations of macroscopic electrodynamics of superconductors in the intermediate state.^[1] In Andreev's theory, the electromagnetic fields were averaged over distances greatly exceeding the dimensions of the normal and superconducting domains that are produced in the sample volume. In this macroscopic approach, to describe the field distributions there is no need to know the structure of the intermediate state, the shape of the domains, the rate of motion of the boundaries, etc. For Andreev's equations^[1] to be valid it is important only that free motion of the domain walls between the phases be possible, i. e., that there be no pinning by the sample defects.

It was shown in^[1] that in a pure uncompensated metal in the intermediate state, just as in the normal state, circularly polarized low-frequency electromagnetic waves—helicons—can propagate in a constant magnetic field. The condition that ensures weak damping of the helicons is a large electron mean free path l in comparison with the characteristic dimensions R of the electron orbits in the magnetic field. Helicons in the intermediate state were first observed experimentally by Maxfield and Johnson in polycrystalline indium samples.^[2] A more thorough investigation was then carried out with lead samples.^[3] In both cases, however, they used pure-quality samples of low-purity metals at $l < R$. This caused a strong damping of the helicons in the intermediate state, which led to difficulties in the interpretation of the experimental results and to apparent discrepancies with the theory.

We report here a detailed experimental investigation of helicons in high-purity indium single crystals. We investigated the dispersion and the damping of the heli-

cons as functions of the magnitude and direction of the magnetic field. All the experimental results obtained in the intermediate state are in full agreement with Andreev's theory.^[1]

HELICON OSCILLATIONS IN A PLATE (THEORY)

1. *Dispersion law.* We consider the distribution of alternating low frequency fields in an unbounded plate of thickness d in the intermediate state. We introduce a system of Cartesian coordinates $(x\eta\xi)$ such that the surfaces of the plate are defined by the equation $\xi = \pm d/2$. We introduce also a coordinate system (xyz) , which is rotated through an angle θ about the x axis relative to the other system, so that the z axis is directed along the constant magnetic field H_0 inside the plate. In the intermediate state $|H_0| = H_c$ (H_c is the critical field) and the connection between the angle θ and the angle φ between the external constant field \mathcal{H} and the ξ axis depends on the value of the field. From the condition that the tangential components of the field intensity be continuous, we get

$$\sin \theta = (\mathcal{H}/H_c) \sin \varphi. \quad (1)$$

The alternating increment to the constant field will be designated by the vector H_1 . We assume that $|H_1| \ll H_c$, and that the dependence of the alternating field on the coordinates and on the time is given by the factor $e^{i\mathbf{k}\mathbf{r} - i\omega t}$. Then as shown in^[1], the following relation should hold between the projection k_z of the wave vector \mathbf{k} on the z axis and the frequency ω :

$$\omega^2 (\sigma_{xy}\sigma_{yx} - \sigma_{xx}\sigma_{yy}) - i\omega \frac{c^2 k_z^2}{4\pi} (\sigma_{xx} + \sigma_{yy}) + \left(\frac{c^2 k_z^2}{4\pi} \right)^2 = 0. \quad (2)$$

Here $\sigma_{\alpha\beta}$ are the components of the conductivity tensor of the metal in the normal state at $H_0 = H_c$, $\alpha, \beta = x, y$.

It follows from Andreev's equations^[1] that the alternating electric and magnetic field intensity vectors lie in a plane perpendicular to H_0 . In pure metals with unequal electron and hole densities $N \neq 0$, under the condition $l \gg R$, we have $\sigma_{xy} \approx -\sigma_{yx} \gg \sigma_{xx} \approx \sigma_{yy}$ and Eq. (2) shows that in the intermediate state there can propagate weakly-damped plane circularly-polarized waves, which were named helicons. Equation (2) coincides with the dispersion law of helicons in a normal metal at $kl \ll 1$ and $\theta = 0$ (see, e. g.,^[4]). The difference lies in the dependence on the angle between k and H_0 . In the normal state Eq. (2) contains besides the projection k_x also the absolute value of k .

2. *Free oscillations.* The natural modes of the oscillations in a sample are obtained from the conditions for the continuity of the tangential components of the magnetic field intensity and the normal components of the magnetic induction on the surface of the sample and the vanishing of the alternating fields as $r \rightarrow \infty$. We note that when solving the external problem we can use the magnetostatic equations, in view of the small dimensions of the sample in comparison with the wavelength in vacuum in the frequency band of interest to us. For an unbounded plate, by virtue of the symmetry of the problem, all the fields depend only on the coordinate ζ , and the boundary conditions reduce to the equality $H_{1x} = H_{1y} = 0$ at $\zeta = \pm d/2$.

Assume that at the initial instant of time $H_{1x} = 0$ and H_{1y} is an even function of ζ . We expand this function in a Fourier series

$$H_{1y} = \sum_k C_k \cos k\zeta.$$

By virtue of the boundary conditions, the wave numbers are $k = n\pi/d$, where n is an odd integer. Taking into account the time dependence, we obtain under the condition $\sigma_{xy}\sigma_{yx} \leq -(\sigma_{xx} - \sigma_{yy})^2/4 \leq 0$:

$$H_{1x} = -\frac{\sigma_{yx}}{\sigma_1} \sum_k C_k \cos k\zeta \sin(\omega' t) e^{-\omega'' t}, \quad (3)$$

$$H_{1y} = \sum_k C_k \cos k\zeta \left(\cos \omega' t + \frac{\sigma_{xx} - \sigma_{yy}}{2\sigma_1} \sin \omega' t \right) e^{-\omega'' t},$$

where

$$\omega' = \frac{c^2 k_x^2}{4\pi} \frac{\sigma_1}{\sigma_2}, \quad \omega'' = \frac{c^2 k_x^2}{4\pi} \frac{\sigma_{xx} + \sigma_{yy}}{2\sigma_2},$$

$$\sigma_1 = [-\sigma_{xy}\sigma_{yx} - (\sigma_{xx} - \sigma_{yy})^2/4]^{1/2}, \quad \sigma_2 = (-\sigma_{xy}\sigma_{yx} + \sigma_{xx}\sigma_{yy})^{1/2},$$

$$k_x = k \cos \theta, \quad k = n\pi/d; \quad n = 1, 3, 5, \dots$$

The vector H_1 executes damped oscillations with a logarithmic damping decrement

$$\Delta = 2\pi\omega''/\omega' = \pi(\sigma_{xx} + \sigma_{yy})/\sigma_1.$$

In the case $|\sigma_{xx} - \sigma_{yy}| \ll |\sigma_{xy}| \approx |\sigma_{yx}|$ the oscillations are circularly polarized, and the direction of rotation of the vector H_1 around the direction of H_0 , coincides with the

direction of rotation of the predominant group of carriers.

As shown by Gaĭdukov^[5] the transverse magnetoresistance ρ for pure indium in a strong field is isotropic, accurate to 5%. For our samples, the critical field at low temperatures is already strong enough. Thus, we can assume that $\sigma_{xx} = \sigma_{yy}$, $\sigma_{xy} = -\sigma_{yx}$. Under these assumptions we obtain

$$\omega' = \frac{c^2 k_x^2}{4\pi} \mathcal{R}_H H_c, \quad \omega'' = \frac{c^2 k_x^2}{4\pi} \rho, \quad \Delta = \frac{2\pi\rho}{\mathcal{R}_H H_c}. \quad (3')$$

Here $\mathcal{R}_H = (Nec)^{-1}$ is the Hall coefficient.

If Δ is not very small, then at equal damping decrements the higher modes of the natural oscillations, corresponding to values $n > 1$, attenuate much more rapidly than the fundamental mode. Thus, after the lapse of a certain time, the distribution of the field in the sample is described by a single exponentially-damped standing wave of frequency ω' , corresponding to the value $k = \pi/d$.

3. *Forced oscillations.* Assume that the alternating field on the surfaces of the plate is specified in the form $H_{1x}(\zeta = \pm d/2) = 0$, $H_{1y}(\zeta = \pm d/2) = H_1 e^{-i\omega t}$, where $\omega = 2\pi\nu$ is a real quantity. Under these boundary conditions, the distribution of the fields inside the plate can be expressed with the aid of the dispersion equation (2) in the form

$$H_{1x} = H_1 \frac{\sigma_{yx}}{2i\sigma_1} \left[\frac{\cos(k\zeta/\cos\theta)}{\cos(kd/2\cos\theta)} - \frac{\text{ch}(k'\zeta/\cos\theta)}{\text{ch}(k'd/2\cos\theta)} \right] e^{-i\omega t},$$

$$H_{1y} = H_1 \frac{1}{2\sigma_1} \left[\left(\sigma_1 + i \frac{\sigma_{xx} - \sigma_{yy}}{2} \right) \frac{\cos(k\zeta/\cos\theta)}{\cos(kd/2\cos\theta)} + \left(\sigma_1 - i \frac{\sigma_{xx} - \sigma_{yy}}{2} \right) \frac{\text{ch}(k'\zeta/\cos\theta)}{\text{ch}(k'd/2\cos\theta)} \right] e^{-i\omega t},$$

$$k = k' + ik'' = (2\pi\omega/c^2)^{1/2} [(\sigma_2 + \sigma_1)^{1/2} + i(\sigma_2 - \sigma_1)^{1/2}].$$

The magnetic flux along the x axis through a sample of unit width is equal to

$$\Phi_x = AC_n (\sigma_{yx}/i\sigma_1) H_1 e^{-i\omega t},$$

where

$$A = \frac{1}{k} \frac{\sin(k'd/\cos\theta) + i \text{sh}(k''d/\cos\theta)}{\cos(k'd/\cos\theta) + \text{ch}(k''d/\cos\theta)} + \frac{i \sin(k''d/\cos\theta) + \text{sh}(k'd/\cos\theta)}{k' \cos(k'd/\cos\theta) + \text{ch}(k'd/\cos\theta)}. \quad (4)$$

Here C_n is the concentration of the normal phase, which is connected with the external field by the relation

$$C_n = (\mathcal{H}/H_c) \cos \varphi [1 - (\mathcal{H}/H_c)^2 \sin^2 \varphi]^{-1/2}.$$

If $|\sigma_2 - \sigma_1| \ll |\sigma_2 + \sigma_1|$, then the first fraction in (4) goes to resonance maxima as the frequency is varied. Enea the maximum of the amplitude Φ_x , the phase difference ψ between the flux and the exciting field H_1 , on the surface of the sample goes through zero. Expressing $\tan \psi = \text{Im} \Phi_x / \text{Re} \Phi_x$ with the aid of formula (4) and retaining only the principal terms, we obtain near the first resonance

$$\tan \psi \approx -(\xi + 0.45\gamma^2 - 0.55\xi^2)/\gamma; \quad (5)$$

$$\xi = (k'd/\pi \cos \theta) - 1, \quad |\xi| \ll 1, \quad \gamma = k''/k'.$$

Neglecting the anisotropy of the transverse magnetoresistance and assuming that $\sigma_{xx} \ll |\sigma_{xy}|$, obtain the relations

$$k' = (4\pi\omega |\sigma_{xy}|/c^2)^{1/2} [1 + 1/8 (\sigma_{xx}/\sigma_{xy})^2] \approx (4\pi\omega/c^2 \mathcal{R}_H H_c)^{1/2} (1 - 3\gamma^2/2); \quad (6)$$

$$\gamma = k''/k' \approx (\sigma_{xx}/2|\sigma_{xy}|) [1 - 1/8 (\sigma_{xx}/\sigma_{xy})^2] \approx \rho/2\mathcal{R}_H H_c.$$

We define the resonant frequency $\nu_0 = \omega_0/2\pi$ in accordance with the condition $\tan\psi = 0$. We then obtain with the aid of (5) and (6)

$$\nu_0 \approx \frac{c^2 \mathcal{R}_H H_c \cos^2 \theta}{8d^2} (1 + 2.1\gamma^2). \quad (7)$$

We note that in contrast to the case of free oscillations, the resonant frequency ν_0 depends on the damping γ .

EXPERIMENTAL PROCEDURE

1. *Samples.* We used in the experiment flat and cylindrical single crystals of indium grown from the melt. Plane-parallel plates with transverse dimensions 8×18 mm and thickness 1 mm were produced in a dismantlable polished quartz mold by the procedure described by Sharvin and Gantmakher.^[6] Two samples (1 and 2) with axes [100] and [011] along the normal n to the plate surface were investigated in greatest detail. The angle between the vector n and the corresponding crystal axis was approximately 5° in both cases.

The cylindrical samples with diameter 4 mm and approximate length 100 mm were cast in glass tubes whose inner walls were coated beforehand with silicon oxide to prevent sticking of the metal to the glass. The single crystals were grown without a primer and their orientations were random. After cooling the metal, the sample was not removed from the glass tube. This protected with extremely soft indium against random deformations. The difference between the temperature coefficients of the glass and the indium made it possible to cool the sample to helium temperatures without producing mechanical stresses.

2. *Measurement setup.* The samples were immersed in liquid helium whose temperature was lowered to 1.2° K. The cryostat was placed between the poles of an electromagnet that produced a homogeneous constant magnetic field \mathcal{H} , which could be rotated in the horizontal plane. The intensity of the field \mathcal{H} in our experiment did not exceed 700 Oe. To register the helicon oscillations we used the known crossed-coil procedure. A system of two excitation coils, placed symmetrically around the cryostat, produced at the location of the sample a small homogeneous field \mathcal{H}_1 directed in the horizontal plane perpendicular to the field \mathcal{H} . In our experiments we had $\mathcal{H}_1 \leq 30$ Oe. A receiving coil ≈ 20 mm long, with vertical axis (x axis), was wound around the sample. The voltage $U \leq 1$ mV induced in the receiving coil was fed to a semiconductor amplifier. The amplified signal was recorded either with an automatic recorder in the case of slow processes, or with a long-persistence oscilloscope in the case of frequencies higher than 1 Hz.

Both free and forced helicon oscillations were excited

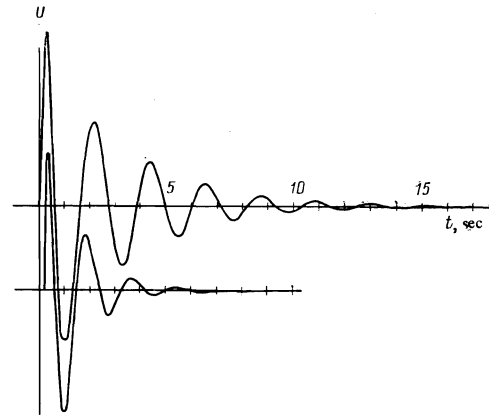


FIG. 1. Plots of free helicon oscillations in a cylindrical sample. The upper curve was plotted in the intermediate state ($C_n = 0.54$, $\mathcal{H} = 185$ Oe), the lower curve—in the normal state ($\mathcal{H} = H_c = 245$ Oe); $T = 1.23$ ° K.

in the experiments. To observe the free oscillations, the constant field \mathcal{H}_1 was turned on or off. The rapid change of the field \mathcal{H}_1 within a time ≈ 0.01 sec excited natural electromagnetic oscillations in the sample, which in turn induced a voltage in the receiving coil. Typical plots of the free helicon oscillations in a cylindrical sample are shown in Fig. 1. With the exception of the initial section, which lasts for approximately half a cycle, the signal is an exponentially decreasing sinusoid corresponding to the fundamental mode of the natural oscillations. The accuracy with which the frequency and the logarithmic damping decrement of the natural oscillations were measured depended strongly on the damping itself, amounting in the best case 2 and 10%, respectively, and in the worst case approximately 10 and 50%.

To observe the forced oscillations, a sinusoidal current of frequency ν was made to flow through the exciting coils. At the start of the experiment, the excitation field \mathcal{H}_1 had to be already oriented perpendicular to the axis of the receiving coil, so as to make the received signal equal to zero in the case when there were no helicons, for example, when the sample went over into the pure superconducting state. In the intermediate and normal states, a voltage U was induced in the receiving coil.

During the course of the experiment we measured the amplitude and the phase of the voltage U as a function of the frequency ν at a fixed field \mathcal{H} . The phase shift ψ_U of the voltage U relative to the excitation field \mathcal{H}_1 was determined from measurements of the Lissajoux figure. To increase the accuracy of the measurements of the quantities $\psi_U \approx \pi/2$, the horizontal sweep of the oscilloscope or of the automatic recorder was fed, when the Lissajoux figure was produced, from a reference voltage source shifted in phase by $\pi/2$ relative to the exciting field \mathcal{H}_1 . The value of ψ_U differed by $\pi/2$ from the phase shift ψ of the flux Φ_x through the sample. The resonant frequency $\nu = \nu_0$ was determined in experiment from the condition $\cot\psi_U = \tan\psi = 0$. The procedure used to observe the forced oscillations and register the resonance by determining the change of the phase turned out to be

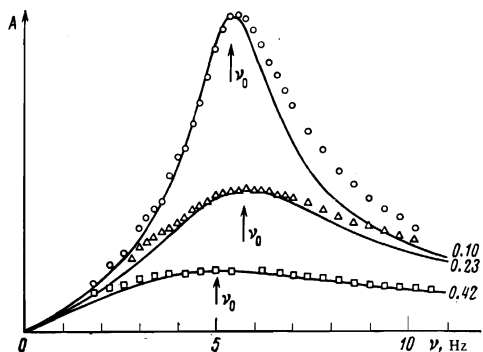


FIG. 2. Resonance curves for induced helicon oscillations. Solid lines—calculation with formula (4) using the experimental values of ν_0 (marked by an arrow) and of the damping γ (indicated on the right side of the curves). Experimental points—results of measurements of the quantity U/ν : \circ — $\mathcal{H} = 100$ Oe, Δ — $\mathcal{H} = 200$ Oe, \square — $\mathcal{H} = 250$ Oe; sample 1, $T = 1.3$ K, $\mathcal{H} \parallel n$. The matching of the vertical scales of the calculated curves and of the experimental points was carried out independently for each curve at one of the values of ν near resonance.

most convenient and most accurate for the study of helicons under strong damping conditions. The reason is that the received signal in this case is larger than in the free-oscillation procedure, and its phase changes more rapidly when the frequency is shifted near the resonance.

EXPERIMENTAL RESULTS FOR FLAT SAMPLES

1. *Shape of resonance curve.* In our experiments we observed only the first resonance. Near the resonance, in accordance with (5), we have

$$\operatorname{tg} \psi \approx (\nu - \nu_0) / 2\gamma \nu_0. \quad (7)$$

On the basis of this relation we determined the damping γ of the helicons from the change in the value of $\tan \psi$ at small detunings $(\nu - \nu_0) / \nu_0 \ll 1$. Just as in the case of the free oscillations, the accuracy of the measurements of the frequency ν_0 and of the helicon damping depended on the value of γ itself. For the smallest values, $\gamma \approx 0.1$, the error in the measurement of ν_0 was $\approx 2\%$, and that of the damping was $\approx 10\%$. For the largest values, $\gamma \approx 0.5$, the error increased by approximately 3 times. Thus, the inaccuracy due to the use of formula (7), from which terms of order γ^2 have been omitted, do not exceed in any case the measurement error. By determining ν_0 and γ we could plot the amplitude A of the quantity Φ_x against the frequency ν in accordance with formula (4). Typical examples are shown in Fig. 2. A comparison of the calculated curves with the measured values of U/ν show that relation (4) describes satisfactorily the shape of the resonance curves for induced helicon oscillations. The amplitude of the helicon signal, in accord with (4), was proportional to the concentration C_n .

2. *Dependence of the dispersion law on the magnetic field.* Figure 3 shows the results of the measurement of the resonance curve ν_0 and the conditional width of the resonance curve $\Delta\nu = 2\gamma\nu_0$ as a function of \mathcal{H} . We discuss first the results obtained at $\mathcal{H} > H_c$.

In the normal state, the helicon dispersion law has the simplest form in the local limits, when the conditions $kR \ll kl \ll 1$ are satisfied. Formula (2) is then valid in the case $\mathcal{H} \parallel n$ for $k_z = k$. The direction of the vector \mathbf{k} inside an unbounded plate, on which an external plane wave is incident, coincides with the normal \mathbf{n} , owing to the large difference between the propagation of velocities of the electromagnetic wave in the metal and in vacuum. By calculations similar to those used in the derivation of (7), we obtain

$$\nu_0 = (c\mathcal{H}/8|Ne|d^2)(1 + 2\gamma^2). \quad (8)$$

The width of the resonance curve $\Delta\nu = 2\gamma\nu_0 \approx \rho c^2/8d^2$ does not depend on the field if we operate under conditions of saturation of the magnetoresistance. According to Gaïdukov's results,^[5] for our samples the change of ρ at $\mathcal{H} \gtrsim H_c$ does not exceed at low temperatures the errors in the measurement of $\Delta\nu$.

In the nonlocal case, when the electron mean free path becomes comparable with or exceeds the wavelength of the helicons, the situation becomes more complicated. However, if the conditions $kR \ll 1$ are satisfied, the connection between the real part of the wave vector and the frequency is given as before by formula (6). At the same time, the damping of the helicons can acquire an additional term connected with the absorption of the wave energy by the electrons that move in phase with the wave, if their orbits are inclined to the constant-phase plane. This is the so-called magnetic Landau damping.^[7] It does not appear if the orbits of the electrons of the central section of the Fermi surface lie in a plane perpendicular to \mathbf{k} . In this case the damping is given as before by formula (6) and the resonance width $\Delta\nu$ does not depend on the field. This is observed in our experiments at $\mathcal{H} \gtrsim 500$ Oe. The values of ν_0 were in this case proportional to \mathcal{H} . The straight lines in Fig. 3 show the extrapolation of these results to weaker fields.

With decreasing magnetic field, the strong inequality $kR \ll 1$ is violated. An important role is then assumed by the nonlocal corrections to the dispersion law, due to the Doppler-shifted cyclotron resonance for electrons moving along the magnetic field (see, e.g.,^[7]). This

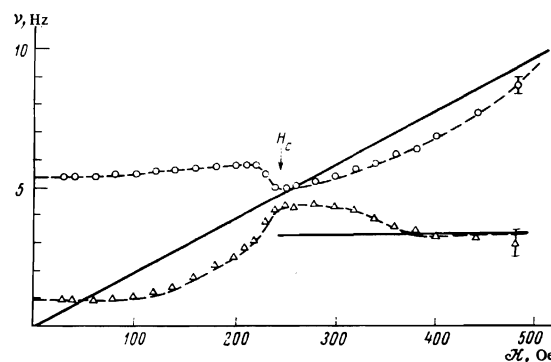


FIG. 3. Dependence of the resonance frequency ν_0 (\circ) and of the conditional width of the resonance curve $\Delta\nu = 2\gamma\nu_0$ (Δ) on the external field. Sample 1, $\mathcal{H} \parallel n$, $T = 1.3$ K. Solid lines—results of extrapolation of the data obtained at $\mathcal{H} > 500$ Oe.

leads to an increase of the helicon damping and to a more complicated $k'(\omega)$ dependence.^[8] These circumstances explain why the experimental points deviate from the straight line on Fig. 3 at $\mathcal{H} > H_c$. In the intermediate state, the electrons move inside the normal domains, being reflected backward from the boundaries with the superconducting phase. The special character of the reflection, in which the quasiparticle excitation branch is changed (electron-hole transition), are the reason why the boundaries between the normal and superconducting phases make no additional contribution to the electric resistance.^[1] As a result of such reflections, however, the electrons become localized inside the normal regions. Therefore all the nonlocal effects that influence the dispersion and the damping of the helicons in the normal state vanish when the characteristic dimension of the normal domains a satisfies the inequality $ka \ll 1$. This condition is in fact the basis of the macroscopic approach itself to the problem of the propagation of helicons in the intermediate states. In our experiments $a \approx 0.1$ mm at $\theta = 0$ and $C_n \approx 0.5$. The most noticeable increase of a takes place at $C_n > 0.9$. According to formula (7), in the intermediate state $\gamma \approx 0$ and $\theta = \varphi = 0$, the value of ν_0 does not depend on the external field. Allowance for the decrease of the damping as $C_n \rightarrow 0$ explains the small changes of ν_0 which are observed in experiment (see Fig. 3).

It should be noted that the limiting value $\nu_0 = 5.3$ Hz, obtained as $C_n \rightarrow 0$, differs noticeably from the value $\nu_0 = 4.9$ Hz which is result of extrapolation of the data from the region of strong fields to the value $\mathcal{H} = H_c$. So appreciable a discrepancy cannot be eliminated by taking into account terms of order $\gamma^2 \approx 0.01$ in the expression for the resonance frequency. Allowance for the corrections necessitated by the finite width of the plate (see, e. g.,^[9]) can make matters only worse, since these corrections should increase the resonance frequency for the sample in the intermediate state to a lesser degree than in the normal state. Although the indicated discrepancy only slightly exceeds the experimental errors, it can serve as evidence that the macroscopic electrodynamics is not accurate. It is possible, that in the approach developed above no account was taken of the role of the sample surface. Near the surface, a change takes place in the relative concentration of the normal and the superconducting phases. This may be why the effective thickness of the sample decreases. We note that the theoretical resonant frequency $\nu_0 = 4.85$ Hz of an infinite plate of thickness 1 mm at $\mathcal{H} = 244$ Oe = H_c (1.3 K) can be obtained with the aid of formula (8) from the value $N = 3.9 \times 10^{22}$ cm⁻³, which corresponds to a carrier density of one hole per atom.

From the experimental data given in Fig. 3 it is evident that the helicon damping is strongly altered by the transition to the intermediate state. The observed decrease of the damping is due to the localization of the electrons inside the normal domains, which leads, first, to a vanishing of the nonlocal cyclotron damping and, second, to a decrease of the contribution of the electron scattering by the sample surface.^[10] We shall assume that at $\mathcal{H} > 500$ Oe the helicon damping is described by formula (6), where the resistivity ρ is determined by a

certain effective electron mean free path $l_{\text{eff}} = (1/l + 1/d)^{-1}$. In this expression, the first term in the right-hand side takes into account the scattering of the electrons in the bulky sample, while the second term takes into account the restriction imposed on the mean free path by the diffuse scattering from the surface of the plate. In the intermediate state the resistivity ρ contains only the bulky-sample mean free path l . These assumptions enable us to estimate l from the ratio of the values of the helicon damping $l/l_{\text{eff}} = 1 + l/d = \Delta\nu(500 \text{ Oe})/\Delta\nu(100 \text{ Oe})$. For sample 1, the value obtained in this manner is $l \approx 3.2$ mm at $T = 1.3$ °K. This value agrees with the estimate of l that can be obtained from the absolute value of the damping of the helicons in the intermediate state $\gamma = \Omega\tau/2$ in accordance with the isotropic-metal model, if we put $l = v\tau$, and if the values of the Fermi velocity $v = 1.1 \times 10^8$ cm/sec and of the cyclotron frequency $\Omega = eH/m^*c$ for an effective mass $m^* = 2m_0$ (m_0 is the mass of the free electron) are taken as the result of averaging of the experimental data over the cyclotron resonance in indium.^[11]

3. *Helicons and structure of intermediate state.* Special experiments were performed to observe the structure of the intermediate state at $\mathcal{H} \parallel n$. These experiments were performed with a magneto-optical setup at the Institute of Experimental Physics (Lausanne) in collaboration with P. Laeng.^[1] The magneto-optical procedure is described in^[12]. As noted earlier,^[13] the structure that arises in the sample is usually far from equilibrium and is determined by the history of the magnetization of the sample, by edge effects, and by other extraneous factors. In particular, Haenssler and Rinderer^[14] have noted that when the field is decreased from the normal state a layered structure is observed in the samples, and when the field is increased from the value $\mathcal{H} = 0$, the intermediate state has a cellular structure. We have arrived at the same conclusion by observing the structure of the intermediate state in our samples. At the same time, the values of the resonance frequency ν_0 and of the helicon damping at $0.3 H_c \leq \mathcal{H} \leq 0.9 H_c$ depended only on the value of the external field, but not on the prior history of the sample magnetization. Thus, one of the main premises of the macroscopic electrodynamics of the intermediate state was confirmed, according to which the Andreev equations, which describe the electromagnetic properties of the intermediate state at low temperatures,^[1] are valid independently of the concrete form of the structure of the normal and superconducting domains.

It is interesting to note that as $\mathcal{H} \rightarrow 0$, when the magnetic flux penetrates into the sample only in individual normal domains that are far from one another, the resonant frequency of the helicon oscillations retains its value. After turning on the external field \mathcal{H} , the process of crowding out the magnetic fields from the sample to the small residual level of the frozen-in field proceeds quite slowly and takes several minutes. In that case ν_0 remains practically constant. All that decreases is the amplitude of the signal in accordance with the decrease of the concentration of the normal phase. These facts agree with the results of the microscopic theory,^[15] which yields for an individual domain the same helicon-

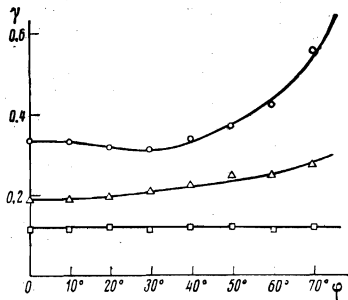


FIG. 4. Dependence of helicon damping on the inclination of the external field: \circ — $\mathcal{H}=250$ Oe, Δ — $\mathcal{H}=200$ Oe, \square — $\mathcal{H}=100$ Oe. Sample 2, $T=1.3^\circ\text{K}$.

oscillation dispersion law as macroscopic electrodynamics.

When the field is smoothly increased, the sample goes over from the pure superconducting state into an intermediate state at $\mathcal{H} \approx 0.3 H_c$. When the structure is visually observed, starting with this value of the external field, a rapid penetration of the normal domains from the edges into the center of the sample begins. In experiments on stimulated helicon oscillations, there is no signal in the receiving coil at $\mathcal{H} < 0.3 H_c$ if the sample was cooled previously from the normal state to a low temperature in a zero field.

At a slight excess of the indicated critical value of the field, the helicon signal reaches rapidly an amplitude corresponding to a specified concentration of the normal phase in a decreasing field. This phenomenon has already been observed in Ref. 3. It is connected with the geometric form of the sample, particularly with the circumstance that the demagnetizing factor of the sample differs from unity. The start of the penetration of the field at $\mathcal{H} \approx 0.3 H_c$ agrees well with the results of the calculation given in^[16].

In the case of a slow decrease of the field from the value $\mathcal{H} = H_c$, a decrease of the frequency ν_0 , which is typical of the normal state, was observed in a number of cases. In the vicinity of the values $\mathcal{H} \approx 0.9 H_c$, uncontrollable factors have caused the resonance frequency to change jumpwise to the value obtained in an increasing field. Thus, in experiments on helicon oscillations we observed a unique supercooling wherein the sample retained the electromagnetic properties of the normal state at $\mathcal{H} < H_c$. It should be noted that it was impossible to observe a similar hysteresis in the vanishing and in the appearance of the traces of the superconducting phase by visual observation of the structure.

4. *Oblique field.* In an oblique field, if the sample is in a normal state under the condition of the local dispersion law, the resonant frequency is $\nu_0 \sim \cos \varphi$, and the damping is $\gamma \sim 1/\cos \varphi$.^[4] In the nonlocal case, the dependences of ν_0 and γ on the angle between \mathbf{k} and \mathcal{H} can be very complicated. An important role is played here by the anisotropy of the Fermi surface. It is very difficult to calculate the changes of the frequency and of the damping under these conditions. This pertains in par-

ticular to the case $kR \approx 1$. On going to the intermediate state, everything simplifies substantially. The electrodynamics again becomes local, and Andreev's formulas make it possible to investigate theoretically the angular dependences.

Let us turn first to helicon damping. According to formula (6), the value of γ does not depend on the angle of inclination of the field. Figure 4 shows experimental data obtained with one of the samples. It is seen that in the normal state the damping is noticeably increased with increasing φ . On going to the intermediate state, this dependence becomes weaker and at a sufficiently high concentration of the superconducting phase the value of γ is independent of the inclination of the vector \mathcal{H} . In the case of sample 1 this situation sets in already at $\mathcal{H} \leq 0.9 H_c$ (see Fig. 5).

In the course of these experiments, measurements were made on two flat samples with random orientation. In the normal state, when the angle φ was varied, there was a complicated interplay in these samples between different factors that determine the helicon damping, while γ had a very unusual nonmonotonic dependence on the angle φ . In the intermediate state at $C_n \approx 0.5$, within the limit of experimental errors, the damping remained constant.

Let us discuss now the changes of the resonant frequency. According to (7), $\nu_0 \sim \cos^2 \theta$. The value of the angle θ can be calculated by using formula (1) from the known values of the angle φ and the ratio \mathcal{H}/H_c . In Fig. 5, the experimental results on the angular dependence of the resonant frequency are represented in coordinates that are convenient for comparison with the theory. As seen from the figure, the theory agrees fully with the measurement results.

HELICON OSCILLATIONS IN A CYLINDER

The problem of the resonance frequencies and of the damping of helicon oscillations in cylinders in a transverse magnetic field presents considerable mathematical difficulties and has not yet been solved. An analysis of the experimental results is presented below to the extent permitted on the basis of the initial equations.

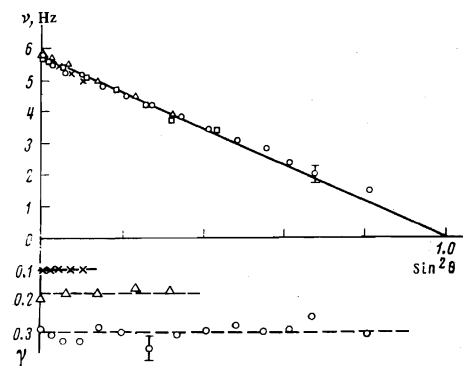


FIG. 5. Dependence of the resonance frequency ν_0 and of the helicon damping γ on the angle θ between the vectors \mathbf{H} and \mathbf{k} : \circ — $\mathcal{H}=220$ Oe, Δ — $\mathcal{H}=180$ Oe, \square — $\mathcal{H}=160$ Oe, \times — $\mathcal{H}=100$ Oe. Sample 1, $T=1.25^\circ\text{K}$.

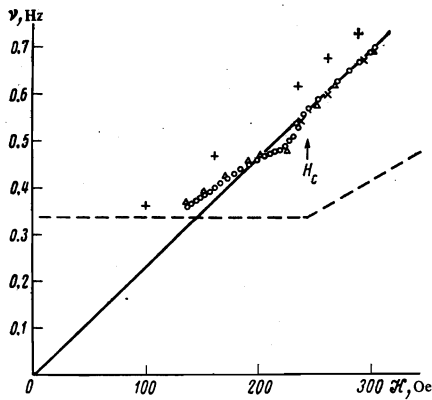


FIG. 6. Dependence of the frequency of the free oscillations (Δ , \times) and of the resonant frequency of the induced oscillations (\circ , $+$) in a cylindrical sample on the field strength. \circ , Δ — $T = 1.23$ K; \times , $+$ — $T = 3.0$ K. The dashed line shows the theoretical dependence for a plate $d = 4$ mm thick. The arrow indicates the field H_c for the low temperature.

Figure 6 shows the results of measurements of the frequency of the free oscillations and the resonant frequency for forced oscillations in a cylindrical sample. As expected, in the case of weak helicon damping these frequencies coincide. All the nonlocal corrections to the helicon dispersion law are nonexistent in view of the large diameter of the cylinder. If the connection between the current density \mathbf{j} and the electric field \mathbf{E} in the normal state is written for the local case in the form

$$\mathbf{E} = \rho \mathbf{j} + \mathcal{R}_H [\mathcal{H} \times \mathbf{j}],$$

then, substituting this relation in Maxwell's equations, we obtain for alternating component of the magnetic field \mathbf{H}_1 the equation

$$\frac{4\pi}{c^2} \frac{\partial \mathbf{H}_1}{\partial t} = \rho \nabla^2 \mathbf{H}_1 - \mathcal{R}_H \text{rot} [\mathcal{H} \times \text{rot} \mathbf{H}_1].$$

It is clear from this equation that at $\rho \ll \mathcal{R}_H \mathcal{H}$ the resonant frequencies for a sample of any shape proportional to \mathcal{H} , while the damping is determined by the ratio $\rho / \mathcal{R}_H \mathcal{H}$.

An estimate of the mean free path of the electrons from measurements of the damping decrement of the free helicon oscillations in cylindrical samples was carried out in^[10] with the aid of formula (3) derived for the case of plane waves. The entire aggregate of the results obtained there makes it possible to assume that the use of formula (3) for the damping decrement in a cylinder does not result in a large error in the data reduction. For the cylindrical sample used in that study, estimates of the electron mean free path in the bulky metal, obtained both with the aid of the isotropic-metal model from the value of the damping as $C_n \rightarrow 0$, and from the change of the damping on going from the normal into the intermediate state with the aid of the simple Nordheim formula (see^[10]) yielded a value $l \approx 6$ mm at $T = 1.23$ °K. Allowance for the temperature dependence of l , which was measured in^[10], yields for the residual mean free path an estimate $l_0 \approx 8$ mm.

In the intermediate state, in the approximation $\rho = 0$, the linearized Andreev equations^[11] yield for the alternating components of the field and for the concentration C_{n1} of the normal phase the relation

$$\frac{\partial \mathbf{H}_1}{\partial t} + \frac{1}{C_n} \mathbf{H}_0 \frac{\partial C_{n1}}{\partial t} = \frac{1}{4\pi} c^2 \mathcal{R}_H \text{rot} (\mathbf{H}_0 \nabla) \mathbf{H}_1. \quad (9)$$

For plane waves, by virtue of the condition

$$C_n \text{div} \mathbf{H}_1 + H_0 \nabla C_{n1} = 0$$

the derivative is $\partial C_{n1} / \partial t \sim C_n \partial H_1 / \partial t$, and Eq. (9) shows that the resonant frequencies of the helicon oscillations in the plate do not depend on the concentration of the normal phase. In the general case this is not so. It appears that this circumstance explains the observed change in the frequency of the natural oscillations in the cylinder with changing external field at $\mathcal{H} < H_c$.

Formulas (3') show that in a plate the frequency of the free oscillations does not depend on the magnitude of the magnetoresistance and remains unchanged so long as the Hall coefficient is constant. At the same time, according to formulas (6), the value of the resonant frequency for the induced oscillations increase with increasing magnetoresistance, i. e., with increasing helicon damping. A similar situation is observed also in a cylinder. Experiments with a cylindrical sample have shown that when the temperature is raised to 3 °K the frequency of the free oscillations in the normal state does not depend on the temperature within the limits of the measurement accuracy, whereas the resonant frequency of the induced oscillations increases noticeably in accordance with the increase of the helicon damping.

The author is grateful to Yu. V. Sharvin and A. F. Andreev for a discussion of the results, to S. V. Gudenko, and L. M. Shpel'ter for help with preparing the samples, and to R. K. Nikolaev and A. D. Bronnikov for supplying high-purity indium.

¹The author takes the opportunity to express sincere gratitude to Professor L. Rinderer for the opportunity of performing the experiments in his laboratory, and due gratitude to P. Laeng, who shouldered the main burden of operating the installation.

¹A. F. Andreev, Zh. Eksp. Teor. Fiz. 51, 1510 (1966) [Sov. Phys. JETP 24, 1019 (1967)].

²B. W. Maxfield and E. F. Johnson, Phys. Rev. Lett. 15, 677 (1965).

³A. Kushnir, W. McLean, A. Kasdan, and B. Maxfield, Phys. Rev. B3, 3812 (1971).

⁴E. A. Kaner and V. G. Skobov, Usp. Fiz. Nauk 89, 367 (1966) [Sov. Phys. Usp. 9, 480 (1967)].

⁵Yu. P. Gaidukov, Zh. Eksp. Teor. Fiz. 49, 1049 (1965) [Sov. Phys. JETP 22, 730 (1966)].

⁶Yu. V. Sharvin and V. F. Gantmakher, Prib. Tekh. Eksp. No. 6, 165 (1963).

⁷P. M. Platzman and P. A. Wolff, Interaction of Solid-State Plasmas, Academic, 1972.

⁸I. P. Krylov, Zh. Eksp. Teor. Fiz. 54, 1738 (1968) [Sov. Phys. JETP 27, 934 (1968)].

⁹C. R. Legendy, Phys. Rev. 135, A1713 (1964).

¹⁰I. P. Krylov, I. L. Bronevoi, and Yu. V. Sharvin, Pis'ma

Zh. Eksp. Teor. Fiz. 19, 588 (1974) [JETP Lett. 19, 306 (1974)].

¹¹R. T. Mina and M. S. Khaikin, Zh. Eksp. Teor. Fiz. 48, 111 (1965) [Sov. Phys. JETP 21, 75 (1965)].

¹²P. Laeng and L. Rinderer, Cryogenics 12, 315 (1972).

¹³J. D. Livingston and W. De Sorbo, Superconductivity, ed. Parks, Vol. II, New York, 1969, p. 1240.

¹⁴F. Haenssler and L. Rinderer, Helv. Phys. Acta 38, 448

(1965).

¹⁵A. F. Andreev, Pis'ma Zh. Eksp. Teor. Fiz. 4, 7 (1966) [JETP Lett. 4, 4 (1966)].

¹⁶J. Provost, E. Paumier, and A. Fortini, J. Phys. F 4, 439 (1974).

Translated by J. G. Adashko

Structure of a polymer globule formed by saturating bonds

I. M. Lifshitz, A. Yu. Grosberg, and A. R. Khokhlov

*Institute of Physics Problems, USSR Academy of Sciences
and Institute for Biological Research on Chemical Compounds; Moscow State University*
(Submitted May 11, 1976)

Zh. Eksp. Teor. Fiz. 71, 1634-1643 (October 1976)

A statistical-thermodynamic analysis is presented of the spatial structure of a long polymer chain in which the loosely-spaced links merge into pairs and form saturated bonds. It is shown that with decreasing temperature such chains form a globular type of structure with irregular joining of the functional links. Although the interaction is by itself incapable of forming a condensed phase, it can lead in a polymer chain to a coil-globule phase transition. The transition is unique in that although formally it is of first order, it is in fact very similar to a second-order transition (the density discontinuity, the heat released, etc. are comparatively small). The extreme cases of a sufficiently short chain in which the excluded monomer volume is of no significance and of an extremely long chain are investigated analytically. A numerical calculation in the intermediate region it has made it possible to fit together the two asymptotic values.

PACS numbers: 36.30.Ba, 61.40.Km

1. INTRODUCTION

The spatial structure of a polymer chain suspended under equilibrium conditions in a dilute solution, is determined by the interactions (direct or via the solvent medium) between the particles of the chain. If these interactions are strong enough, then they stabilize various structure elements, as a result of which, depending on the concrete character of the acting forces, the polymer coils can turn into globules, helices, folded structures, etc.

The interactions of the parts of the chain with one another and with particles of the solvent are divided into two qualitatively different classes: saturated bonds (covalent, hydrogen) and unsaturated (van der Waals, multipole, etc.). It is known that unsaturated forces lead, with decreasing temperature, to formation of globules of various types. On the other hand, in the case of saturating bonds, the resultant structure depends essentially on the character of the arrangement of the functional (capable of forming bonds) monomers along the chain.

Whereas all the monomers of the chain, or at least those that are densely arranged along it, are capable of forming bonds, a regular conformation of the helical or folded type is thermodynamically not profitable; examples are the α helix or the β structure of polypeptides. In essence, the reason why such regular structures are thermodynamically favored is the rigidity of the section of the chain between the neighboring functional groups,

as a result of which the entropy loss occurring when a definite conformation is fixed is small.

The opposite case, however, wherein the functional units are quite widely spaced and are separated by flexible pieces of chain, is also possible (the distance between these pieces along the chain is larger than or of the order of the so-called persistence length, i.e., the length over which the memory of the direction is lost). In this situation, any structure with a definite fixed method of binding the pieces of the chain is entropywise unprofitable, so that the chain should (with decreasing temperature) form a structure of the globular type, in which most closed bonds are made up of particles that are very widely spaced along the chain.

This paper is devoted to an analysis of the spatial structure of the globule and of the coil-globule phase transition in such systems.

Under conditions when the functional groups are separated by long sections of a "nonfunctional" chain, it is natural to assume that the length of the bond between two linked ("reacting") groups is small in comparison with the length of the "nonfunctional" section. We can therefore employ the formalism developed in^[1] and^[2] for a statistical-thermodynamics description of the polymer chain with short-range (in the sense indicated above) forces of lateral interaction. We recall that an essential feature of this formalism was the method of introducing into the theory a concrete form of lateral interaction: all the results were expressed in terms of thermody-